CHEMISTRY
AN ASIAN JOURNAL

DOI: 10.1002/asia.200900412

Preparation and Characterization of Chiral Oxazaborolidine Complex Immobilized SBA-15 and Its Application in the Asymmetric Reduction of Prochiral Ketones

Umesh Balakrishnan,[a, b] Nallamuthu Ananthi,[b] Sakthivel Tamil Selvan,[a] Ravindra Pal,[a] Katsuhiko Ariga,[a] Sivan Velmathi,*[a, b] and Ajayan Vinu*[a]

Abstract: The immobilization of chiral oxazaborolidine complex in the well-ordered mesochannels of SBA-15 is demonstrated by a postsynthetic approach using 3-aminopropyltriethoxysilane as a reactive surface modifier. The immobilized catalysts are characterized by various techniques, such as XRD, nitrogen adsorption, HRSEM, UV/Vis diffuse reflectance spectroscopy, and FTIR spectroscopy. The catalysts are used for the enantioselective reduction of aromatic prochiral ketones. The activity of the chiral oxazaborolidine complex immobilized SBA-15 catalysts is also compared with that of the pure chiral oxazaborolidine complex, which is a homogeneous catalyst. It is found that the activity of the chiral complex immobilized SBA-15 heterogeneous catalyst is comparable with that of the homogeneous catalyst.

Keywords: asymmetric catalysis · ketones · mesoporous materials · reduction · silicates

Introduction

Chiral secondary alcohols are important intermediates for the synthesis of chiral natural products and biologically active compounds.[1] Among the various methods available for the synthesis of secondary alcohols, the enantioselective reduction of prochiral ketones with borane in the presence of a chiral ligand is one of the efficient methods, and has received considerable attention in recent years. The pioneering works of Itsuno and co-workers[2,3] and Corey and co-workers[4–8] have inspired the research interest of chemists in the asymmetric reduction of prochiral ketones to chiral secondary alcohols using chiral oxazaborolidines derived from borane and homogeneous catalysts starting from chiral amino alcohols. Several reports focus on the preparation of chiral ligands with different functional moieties and their catalytic activity under homogeneous conditions.[9,10] However, homogeneous catalysts have several drawbacks, such as the difficulty in separation of products from the reaction mixture, wastage of expensive chiral ligands, tedious workup, and rigorous reaction conditions, which limit their usage in industry. To avoid these problems, the conversion of the homogeneous system into a heterogeneous phase by immobilizing the chiral ligands in a solid matrix is highly critical and interesting.

Yao et al. used organic polymers and silica materials as the support for the immobilization of homogeneous asymmetric catalysts and studied their chiral activity.[11] Unfortunately, these supports have poor textural parameters and could not accommodate a huge quantity of the chiral ligands, which is critical for various applications. Recently, mesoporous MCM-41 materials with various pore diameters, which offers large surface areas and uniform pore size distribution, were used as the supports for the immobilization of amino alcohol derivatives and their catalytic properties were investigated in the asymmetric reduction of ketones.[12–16] However, these materials suffer from poor thermal and polar solvent stability. Thus, it is highly imperative to find supports that are thermally and water stable. The highly ordered, large-pore mesoporous silica molecular sieve SBA-

[a] U. Balakrishnan, S. T. Selvan, Dr. R. Pal, Dr. K. Ariga, Dr. S. Velmathi, Dr. A. Vinu
International Center for Materials Nanoarchitectonics
World Premier International (WPI) Research Initiative
National Institute for Materials Science
Tsukuba, Ibaraki 305-0044 (Japan)
Fax: (+81) 29-860-4706
E-mail: vinu.ajayan@nims.go.jp

[b] U. Balakrishnan, N. Ananthi, Dr. S. Velmathi
Organic and Polymer Synthesis Laboratory
Department of Chemistry
National Institute of Technology
Tiruchirappalli-620 015 (India)

15, which has considerably thicker pore walls than MCM-41, was recently synthesized by using an amphiphilic triblock copolymer as the structure-directing agent in highly acidic media.[17] SBA-15 exhibits improved hydrothermal and water stability relative to MCM-41.[18,19]

Herein we demonstrate for the first time the immobilization of chiral oxazaborolidine complex on the porous matrix of highly ordered, hexagonal-type, two-dimensional mesoporous silica SBA-15 by a postsynthetic approach using 3-aminopropyltriethoxysilane as a reactive surface modifier. The immobilized catalyst was characterized by several physicochemical techniques to prove that the chiral complex is perfectly immobilized in the mesochannels of SBA-15. The catalysts were tested for the enantioselective reduction of aromatic prochiral ketone. It was found that the immobilized catalyst show similar activity as that of the homogeneous catalysts in the above reaction. Further, it was found that the chiral complex immobilized SBA-15 is more stable than the pure chiral complex.

Results and Discussion

Synthesis and Characterization of (*R*,*E*)-Alkyl 2-(5-chloro-2-hydroxybenzylamino)-3-methyl butanoate (CAL) Immobilized SBA-15

The first step in the preparation of (*R*,*E*)-alkyl 2-(5-chloro-2-hydroxybenzylamino)-3-methyl butanoate (CAL) immobilized SBA-15 is the covalent grafting of aminopropyltriethoxysilane (APTES) groups on the surface of the pore wall structure of SBA-15. This process introduces amine groups on the surface of the pore walls, which is required for anchoring the CAL (Scheme 1). Elemental analysis confirmed that the APTES-modified SBA-15 contains a significant amount of carbon and nitrogen, proving that the APTES groups are covalently bound to the surface silanol groups of SBA-15. The APTES-modified SBA-15 was further treated with CAL to form CAL-immobilized SBA-15, a heterogeneous chiral catalyst. After the encapsulation, the catalyst was washed several times with different solvents until no more CAL was detected in the supernatant of the washing solvent. It has been reported that the unreacted surface silanol groups on the modified mesoporous catalyst significantly affect the enantioselectivity of a given chiral reaction.[20] Thus, it is imperative to cap the unreacted surface silanol groups with trimethyl silyl (TMS) groups after the encapsulation of the CAL. As shown in Scheme 1, CAL-immobilized SBA-15 was treated with hexamethyldisiloxane (HMDS) to cap the free surface silanol groups with TMS groups.

To understand the degree of CAL encapsulation and the structure of the SBA-15 support after CAL immobilization, the immobilized catalyst was characterized by XRD, nitrogen adsorption, and HRSEM studies. Figure 1 shows the

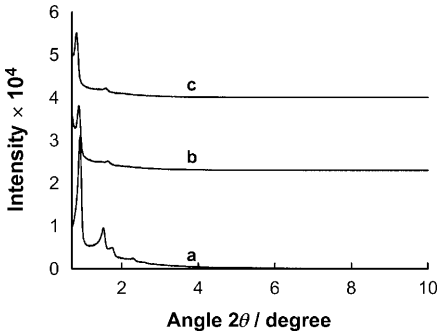

Figure 1. Powder XRD patterns of a) pure SBA-15, b) APTES-functionalized SBA-15, and c) CAL-immobilized SBA-15.

powder XRD patterns of pure SBA-15, APTES-functionalized SBA-15, and CAL-immobilized SBA-15. All the samples show a well resolved (100) reflection and several higher order reflections at 2θ angles between 1.5 and 3°, indicating excellent structural ordering with *p6mm* space group symmetry, and the XRD patterns are similar to that of the previously reported pure SBA-15 silica material. This result indicates that all the materials, even after the modification with amine or CAL, exhibit well ordered two-dimensional hexagonal structures with linear arrays of pores arranged in regular intervals. It is interesting to note that the intensity of the peaks at lower angle for the amine-, and CAL-immobilized SBA-15 is much lower than that of the parent SBA-15 without any modification. The reduction in the intensity of the peaks mainly arises from the encapsulation of the CAL or APTES groups on the surface, which gives the large contrast in density between the silica walls and the empty pores relative to that between the silica walls and the functional molecules, which are attached on the porous surface

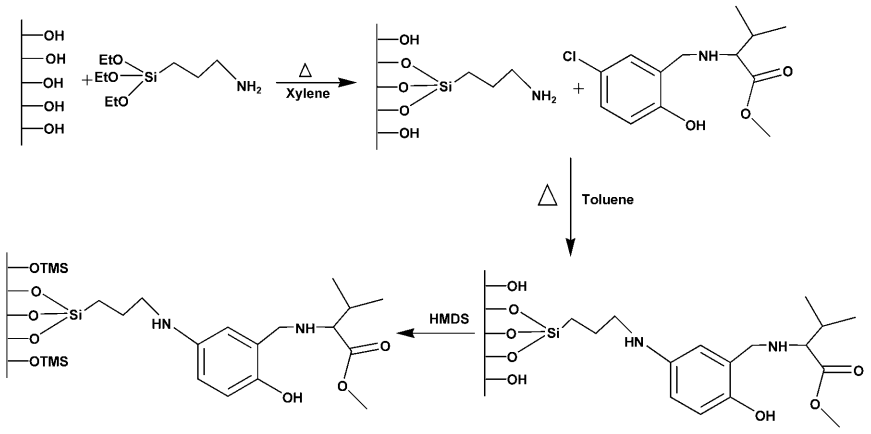

Scheme 1. Preparation of CAL-immobilized SBA-15 end capped with TMS.

CHEMISTRY
AN ASIAN JOURNAL

of SBA-15. These results also confirm that the CAL is immobilized inside the mesochannels of SBA-15.

Figure 2 shows the nitrogen-adsorption isotherms of pure SBA-15 as well as amine- and CAL-immobilized SBA-15, and the results for those samples are given in Table 1. As expected, the modification of the SBA-15 support with amine or CAL caused a significant change in the textural parameters of the support. The amount of nitrogen adsorbed significantly decreased after modification of the porous surface of SBA-15 with amine or CAL, revealing that the specific surface area and pore volume of the support are lower than those of the parent SBA-15 (Table 1). It was found that the capillary condensation step in the isotherms of amine and CAL immobilized SBA-15 was shifted towards lower relative pressure, indicating that pore size of the support is also significantly decreased after the modification. The decrease in surface area, pore volume, and the pore diameter (Figure 3) of the immobilized sample is not related to the collapse of the structural order of the materials during the modification process but instead demonstrates that the CAL molecules are immobilized inside the mesopore channels of the SBA-15 support. In addition, the sharpness of the capillary condensation step and the shape of the hysteresis loop in the nitrogen adsorption isotherm are similar to those of the pure SBA-15, further confirming that the order of the mesopore structure of the support is retained even after modification with CAL. These results are also in good agreement with the data obtained from the XRD measurements of the CAL immobilized SBA-15.

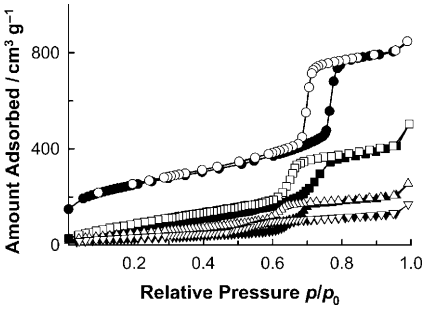

Figure 2. Nitrogen adsorption (filled)–desorption (empty) isotherms of pure SBA-15 (●), APTES-functionalized SBA-15 (■), CAL-immobilized SBA-15 (▲), and CAL-immobilized SBA-15 capped with TMS groups (▼).

Table 1. Textural characterization of pure mesoporous silica SBA-15 and CAL-immobilized SBA-15.

Catalyst	BET surface area [$m^2 g^{-1}$]	Total pore volume [$cm^{-3} g^{-1}$]	BJH pore diameter [nm]
SBA-15	895	1.20	9.0
APTES-functionalized SBA-15	304	0.64	6.9
CAL-immobilized SBA-15	176	0.32	6.7
CAL-immobilized SBA-15 end capped with TMS groups	108	0.20	5.7

The CAL-immobilized SBA-15 materials were characterized by FTIR spectroscopy to further prove the anchoring

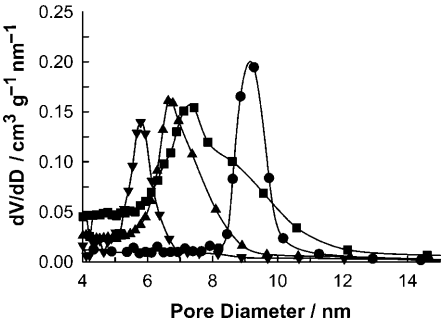

Figure 3. Pore size distribution of pure SBA-15 (●), APTES-functionalized SBA-15 (■), CAL-immobilized SBA-15 (▲), and CAL-immobilized SBA-15 capped with TMS groups (▼).

of CAL inside the mesoporous channels of SBA-15 support. The results were also compared with the spectra of pure SBA-15 and CAL. Figure 4 shows the FTIR spectra of pure CAL and CAL-immobilized SBA-15 catalyst with and without capping. As can be seen in Figure 4, the typical vibration modes of SBA-15 at 3328 cm^{-1} for OH, around 1076 cm^{-1} for Si–O–Si, and a sharp peak at 945 cm^{-1} for Si–OH were present in the case of both pure SBA-15 (Figure 4b) and amine-functionalized SBA-15 (Figure 4c). In the case of amine-functionalized SBA-15, a small shoulder at 2934 cm^{-1}, which is ascribed to the CH stretching frequency of the aminopropylate triethoxysilane, and a peak at 1515 cm^{-1}, which is assigned to NH bending, were observed. It can also be seen from Figure 4 that a number of sharp vibrational peaks observed in the ranges 3100–2900 cm^{-1} and 1200–800 cm^{-1} for pure chiral ligand. Both the amine-functionalized and CAL-immobilized SBA-15 (Figure 4c,d) show the bands in the range of 2900–3400 cm^{-1} and 1200–800 cm^{-1}. The shoulder at 1735 cm^{-1} is attributed to the ester carbonyl group of chiral catalyst, confirming the presence of CAL groups, which are perfectly anchored with the amine-modified SBA-15, even after repeated washing with dichloromethane in the

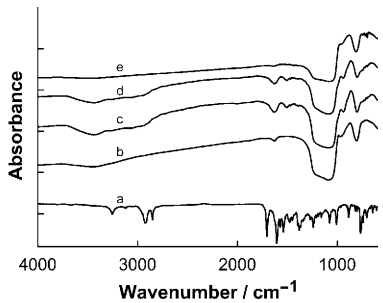

Figure 4. FTIR spectra of a) pure CAL, b) pure SBA-15, c) APTES-functionalized SBA-15, d) CAL-immobilized SBA-15, and e) CAL-immobilized SBA-15 capped with TMS groups.

preparation process. However, most of the peaks related to the pure chiral ligand were not observed for the chiral ligand loaded SBA-15 support. This could be attributed to the confinement or shielding effect of the mesoporous silica framework of the SBA-15 support by the vibration of chiral ligand **1** (see Scheme 2). This result confirms that the pure chiral catalyst is anchored inside the pores and not simply doped or physisorbed on the external surface of the SBA-15 support. It is interesting to note that the intensity of the OH band significantly decreases after an end-capping process, confirming that the free surface silanol groups present in the pore walls of CAL immobilized SBA-15 are capped with TMS groups (Figure 4).

The stability of the CAL groups inside the mesochannels of SBA-15 was investigated by UV/Vis diffuse-reflectance spectroscopy (DRS). Figure 5 shows the UV/Vis DRS spectra of pure SBA-15 and CAL-immobilized SBA-15. Pure chiral ligand **1** exhibits two sharp bands in the UV spectrum centered at 290 and 235 nm. The peak at 235 nm is attributed to a π–π* transition, whereas the peak at 290 nm is assigned to an n–π* transition. The intensity of the bands for CAL-immobilized SBA-15 is much lower than that for pure CAL. This is mainly on account of the low concentration of ligand in the mesochannels of SBA-15. Also, there was a slight shift in absorption frequency, which can be attributed to the inducement interaction between NH group and catalyst and the arrangement of the chiral ligands in the well-ordered mesopore channels of the SBA-15 support, confirming that ligands are perfectly immobilized inside the mesochannels and are highly stable even after immobilization.

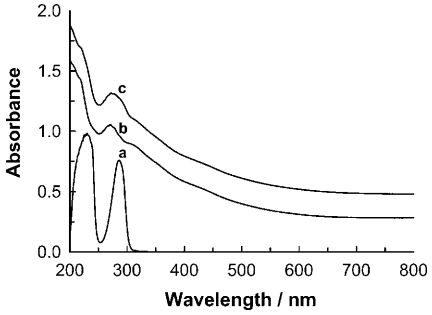

Figure 5. UV/Vis DRS spectra of a) pure CAL, b) CAL-immobilized SBA-15, and c) CAL-immobilized SBA-15 capped with TMS groups.

The morphology of SBA-15 before and after CAL modification was analyzed by HRSEM. Figure 6 shows the HRSEM images of the SBA-15 support before and after the CAL encapsulation at low and high resolution. Both samples exhibit rodlike particles that are uniform in size and shape and aggregated as bundles. It is important to note that the structure and the morphology of the materials were not affected by modification with CAL. These results are also in agreement with the XRD and nitrogen-adsorption data. From all these results, it can be concluded that the SBA-15 support is highly robust owing to its thick walls and is an excellent support for the immobilization of different functionalities inside the mesochannels.

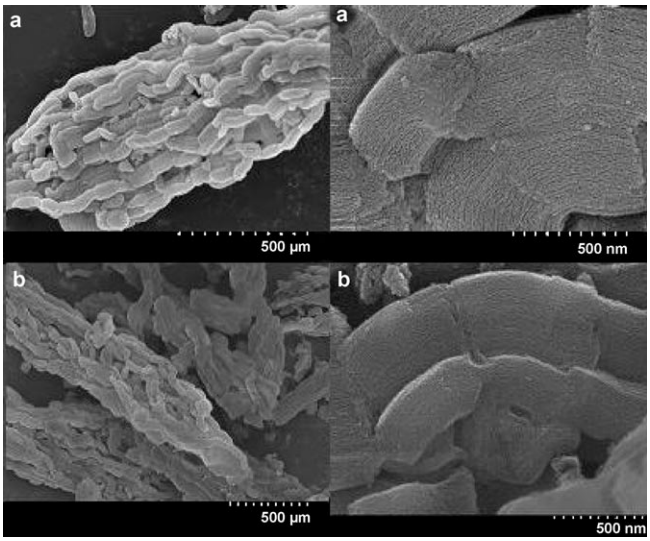

Figure 6. HRSEM images of a) pure SBA-15 and b) CAL-immobilized SBA-15 at low (left) and high (right) resolution.

Catalytic Performance of Pure CAL

We previously reported the synthesis of the amine ester of salicylaldehyde with L-valine and studied the prochiral ketone reduction reaction in stoichiometric quantity with an enantioselectivity of 90% with a product yield of 95%.[21–23] Herein we demonstrate the use of CAL, the same ligand with a halide substitution in amine esters of salicylaldehyde, with the aim of linking the ligand on the surface of the mesoporous SBA-15 support and studying the borane reduction in catalytic amounts under different reaction conditions (Scheme 2).

The homogeneous reduction of acetophenone was carried out as a model reaction to optimize the reaction conditions (Scheme 3; Table 2). The enantioselectivity of borane reduction may be affected by reaction conditions such as solvent and reaction temperature.[24,25] As it has been reported that THF is the better solvent than toluene and dichlorome-

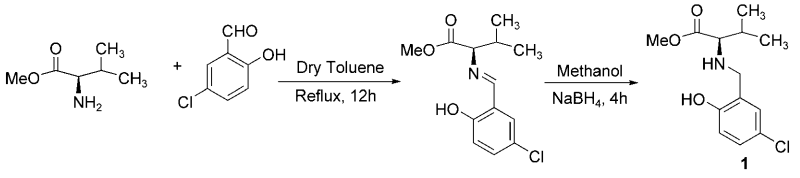

Scheme 2. Synthesis of chiral oxazaborolidine complex **1**.

CHEMISTRY
AN ASIAN JOURNAL

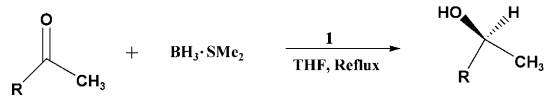

Scheme 3. Asymmetric reduction of prochiral ketones.

Table 2. Reduction of acetophenone with 30 mol % CAL.

Entry	Ligand	Catalyst concentration [mol %]	T [°C]	Yield [%]	*ee* [%][a]	Absolute configuration[b]
1	**1**	30	−77	100	0	racemic
2	**1**	30	0	98	0	racemic
3	**1**	30	35	99	10	*S*
4	**1**	30	65	100	92	*S*

[a] The enantiomeric excess was determined using a chiralcel OD-H column. [b] The absolute configuration was determined by the sign of the optical rotation.

thane,[26] THF was used as the solvent in this study. As can be seen in Table 2, the reaction temperature (−78 °C, 0 °C, room temperature, refluxing conditions) has a profound effect on the enantioselectivity of the product. As the reaction temperature is increased from −77 to 65 °C, the enantioselectivity to the chiral secondary alcohol increases from 0 to 92 % for the reduction of acetophenone with 30 mol % of pure CAL. The product enantioselectivity is 0 at low temperature, which is attributed to the formation of a dimer of oxazaborolidine.[8] Another factor is that at low temperature (0 °C), the equilibrium could be shifted more towards the intramolecular ester carbonyl coordination with boron, which does not facilitate the selective reduction of ketone, leading to a low enantioselectivity. In contrast, at reflux temperature, the equilibrium would be shifted more towards the ketone carbonyl coordination with boron, which aids more selective reduction of the ketone and is thus responsible for a high enantioselectivity.

The instantaneous reduction indicates that the reduction is effected by nitrogen-coordinated borane ($N{-}BH_3$), which is more nucleophilic. The predominant formation of the *S* enantiomer may arise from the more selective transfer of hydride from the reagent to the *Si* face of the ketone. Hence, Corey's mechanism involving the hydride transfer from the reagent to the ketone through the formation of a six-membered cyclic transition state is expected for the reduction. However, the lower observed *ee* value for the reduction may be a result of the competition of the carbonyl group of the ketone for coordination with boron from the ester carbonyl of the reagent (Scheme 4).

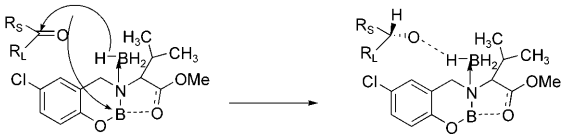

Scheme 4. Reduction of acetophenone by chiral oxazaborolidines.

Catalytic Performance of CAL-immobilized SBA-15 in the Asymmetric Reduction of Prochiral Ketones

Reduction of acetophenone was carried out with CAL-immobilized SBA-15 (30 mol %) dissolved in dry toluene. Borane dimethylsulfide (0.12 mL, 1.5 mmol) was added dropwise, and the mixture was heated at reflux for 30 min. Acetophenone (0.12 mL, 1 mmol) was added dropwise, and the mixture was heated at reflux for a further 30 min (Table 3, entry 1). Subsequently, the reaction mixture was cooled to room temperature and filtered. To the filtrate 2 N HCl was added, and the product was extracted with dichloromethane. The secondary alcohol was separated by column chromatography with silica gel as adsorbent with 98:2 hexane/ethyl acetate as eluant. However, the alcohol obtained was racemic, possibly because the free OH groups on the silica surface could catalyze the reaction. Hence, the acetophenone reduction was carried out with CAL-immobilized SBA-15 end capped with TMS groups (Table 3, entry 2). As expected, the enantioselectivity was increased to 70 %. Thus, the reduction of aromatic ketones was studied with CAL-immobilized SBA-15 end capped with a TMS group (Table 3). *p*-Bromoacetophenone gave excellent enantioselectivity of 98 %, whereas other ketones, except for *p*-methylacetophenone, gave moderate enantioselectivity (53–86 %).

Table 3. Reduction of aromatic ketones with CAL-encapsulated SBA-15 end capped with TMS groups.

Entry	Ketone	Catalyst concentration [mol %]	T [°C]	Yield [%]	*ee* [%][a]	Absolute configuration[b]
1	acetophenone[c]	30	105	30	0	racemic
2	acetophenone	30	105	90	70	*S*
3	*p*-OMe acetophenone	30	105	38	60	*S*
4	*p*-I-acetophenone	30	105	76	86	*S*
5	*p*-Br-acetophenone	30	105	40	98	*S*
6	*p*-NH_2-acetophenone	30	105	35	53	*S*
7	*p*-Me-acetophenone	30	105	35	4	*S*
8	1st recovery[d]	30	105	80	45	*S*
9	2nd recovery	30	105	44	28	*S*
10	3rd recovery	30	105	40	25	*S*

[a] The enantiomeric excess was determined using a chiralcel OD-H column. [b] The absolute configuration was determined by the sign of the optical rotation. [c] Reaction was performed with CAL-immobilized SBA-15 without end capping. [d] Reduction with acetophenone.

The catalyst was separated from the product mixture and reused to study its recyclability. The recovered chiral catalyst shows lower enantioselectivity and product yield than those of fresh CAL-immobilized SBA-15 end capped with TMS group (Table 3, entry 8–10). This decreased performance could be as a result of the repeated washing of the catalyst with methanol, which may change the active sites from B–H to B–OMe. B–OMe is comparatively less reactive than the B–H for reduction. In addition, this conversion process may also affect the number of actives sites available for the reaction, which leads to low enantioselectivity and product yield. It should be noted that removing the unreacted reactant and product molecules adsorbed on the mesochannels of the SBA-15 without affecting the active sites of the CAL is a challenging task and encompasses a different scope to that of this study. We are in the process of stabilizing the catalyst after the reaction with a different approach that requires a lot of time, and the results will be reported in the future.

Conclusions

The immobilization of chiral oxazaborolidine complex on the porous matrix of highly ordered, hexagonal-type, two-dimensional mesoporous silica SBA-15 by a postsynthetic approach using 3-aminopropyltriethoxysilane as a reactive surface modifier has been demonstrated. The immobilized catalyst is perfectly anchored in the mesochannels of SBA-15. Both the homogeneous and the heterogeneous catalytic activity of the chiral oxazaborolidine ligand for the enantioselective reduction of aromatic prochiral ketones were investigated. It was found that the immobilized catalyst shows similar activity to that of the homogeneous catalyst in the above reaction. However, the enantioselectivity of the catalyst decreases with repeated recycling experiments.

Experimental Section

Chemicals were purchased from Aldrich and used without further purification. Solvents were purchased from Merck and used after purification. The chiral ligands were prepared under nitrogen atmosphere.

Synthesis of L-valine methyl ester hydrochloride: L-Valine (2 g, 17.1 mmol) was dissolved in methanol (20 mL). Thionyl chloride was added dropwise with stirring at 0 °C, and stirring was continued overnight. The final product (2.8 g, 100% yield) was obtained by removing the excess thionyl chloride by rotary evaporation. M.p.: 171–173 °C; $[\alpha]_{25}^{589} = +26.6°$ ($c = 5$ in water); IR (cm^{-1}) 3340, 2900, 1736, and 1235; ^1H NMR ($CDCl_3$): $\delta = 8.4$ (s, 2H, $-NH_2$), 3.7–3.73 (d, 1H,-CH), 3.8 (s, 3H, $-OCH_3$), 2.1–2,2 (s, 1H, -CH), 0.9 ppm (m, 6H, $-(CH_3)_2$; ^{13}C NMR ($CDCl_3$): $\delta = 17.68$, 18.28, 28.97, 38.80, 40.06, 57.23, 170.06 ppm.

Synthesis of (*R*,*E*)-methyl 2-(5-chloro-[2-hydroxybenzylidene]amino)-3-methylbutanoate: L-Valine methyl ester hydrochloride (2 g, 12.075 mmol) was dissolved in dry toluene, and triethylamine (2 mL) and 5-chlorosalicylaldehyde (1.89 g, 12.075 mmol) dissolved in dry toluene were added. The reaction mixture was heated at reflux for 12 h. Finally, a yellow solid product imine (3.15 g, 11.53 mmol) was obtained by removing the excess solvent. M.p.: 71–72 °C, $[\alpha]_{25}^{589} = -96.6°$ ($c = 1$ $CHCl_3$); IR: $\tilde{\nu} = 3432$, 2923, 1737, 1630 cm^{-1}; ^1H NMR ($CDCl_3$): $\delta = 0.84$ (d, 6H, $-(CH_3)_2$), 2.23 (m, 1H, -CH), 3.71–3.74 (d, 1H, -CH,), 3.76 (s, 3H, $-OCH_3$), 6.3–7.25 (m, 3H, Ar), 8.36 (s, 1H, -CH=N), 10.08 ppm (s, 1H, -OH); ^{13}C NMR ($CDCl_3$): $\delta = 18.13$, 18.39, 30.94, 45.85, 52.23, 110.1, 119.9, 126.7, 133.8, 135.4, 160.2, 165.3, 171.3 ppm; MS: *m*/*z* 269, 254,226, 210, 166.

Synthesis of (*R*,*E*)-methyl 2-(5-chloro-2-hydroxybenzylamino)-3-methylbutanoate: The imine (2 g, 7.359 mmol) was dissolved in methanol, cooled to 0 °C, and then sodium borohydride (1 g) was added. The reaction mixture was stirred for 5 h and then quenched by adding 20 mL of 2.5 M HCl. The chiral amine (1.8 g, 80% yield) was obtained by extraction of the resultant mixture with diethyl ether, followed by the purification by column chromatography using silica gel as an adsorbent with 90:10 hexane/ethyl acetate. Hereafter, (*R*,*E*)-alkyl 2-(5-chloro-2-hydroxybenzylamino)-3-methylbutanoate is denoted as CAL. $[\alpha]_{25}^{589} = -82°$ ($c = 0.4$, methanol); IR: $\tilde{\nu} = 3300$, 2950, 1742, 1595, 1280, 1230 cm^{-1}; ^1H NMR ($CDCl_3$): $\delta = 0.89$ (d, 6H, $-(CH_3)_2$), 2.01 (m, 1H, -CH), 3.1(d. 1H, -CH), 3.67 (s, 3H, $-OCH_3$), 3.93 (d, 1H, -CH), 5.22 (s, 1H, -CH), 6.67,6.74 (d, 1H, aromatic), 6.74 (s, 1H, aromatic), 6.88–7.07 ppm (d, 1H, aromatic); ^{13}C NMR: $\delta = 18.21$, 19.35, 31.36, 51.56, 51.81, 65.93, 116.43, 119.24, 122.26, 128.6, 129.03,157.8, 174.11 ppm; MS: *m*/*z* 270, 254, 239, 212, 185, 158.

Synthesis of SBA-15: Highly ordered mesoporous SBA-15 support was synthesized by the procedure previously reported by Zhao et al.[14] under hydrothermal conditions using a triblock organic copolymer as a template. In a typical synthesis, triblock copolymer (4 g), poly(ethylene oxide)–poly(propylene oxide)–poly(ethylene oxide) (EO_{20}-PO_{70}-EO_{20}) (Pluronic P123, MW = 5800) was dispersed in doubly distilled water (40 g) and 2 M aqueous HCl (120 mL) was added with stirring at ambient temperature (35 °C) for 3 h. Finally, tetraethylorthosilicate (4 g) was added to the homogeneous solution with stirring at 40 °C for 24 h to form a gel. The resultant gel was allowed to stand at 100 °C for 48 h in a Teflon Parr reactor, which led to crystallization under static hydrothermal conditions. The white solid product was filtered off, washed with warm distilled water several times, and dried at 150 °C overnight. The as-synthesized solid product was calcined at 540 °C in air for 24 h to remove the organic template.

Preparation of 3-aminopropyltriethoxysilyl-functionalized SBA-15: A suspension of aminopropyltriethoxy silane (APTES) (0.45 g, 2 mmol) and calcined SBA-15 (1 g) in toluene (20 mL) was heated at reflux with continuous stirring under an inert atmosphere for 24 h. The resulting mixture was cooled to room temperature, filtered, washed with dry toluene and diethyl ether, and then dried under vacuum at ambient temperature. The dried material was further subjected to Soxhlet extraction with dry dichloromethane for 24 h to remove the unreacted APTES. Finally, the functionalized SBA-15 solid product was dried at 70 °C under vacuum for 12 h.

Heterogenization of (*R*,*E*)-alkyl 2-(5-chloro-2-hydroxybenzylamino)-3-methylbutanoate on aminopropyl-functionalized SBA-15: The immobilization of CAL in the pore channels of APTES-functionalized SBA-15 was carried out by adding APTES-functionalized SBA-15 (1 g) and CAL (0.2 g, 0.74 mmol) in dry toluene (20 mL). The resulting suspension was heated at reflux for 48 h under inert atmosphere. The CAL-immobilized supported catalyst was filtered, washed thoroughly with dry toluene and diethyl ether, and extracted repeatedly with methanol and dichloromethane in a Soxhlet extractor until the washings become colorless in order to remove unreacted or physisorbed CAL from the pore surface of the functionalized SBA-15. All washings were combined, the solvent was evaporated, and the residue was dissolved in methanol (20 mL). The degree of loading of CAL inside the pore channels of SBA-15 was calculated by subtracting the amount found by UV absorption in the final solution after immobilization from the amount of CAL present before addition of the functionalized SBA-15 support.

Trimethylsilylation (TMS) of CAL-immobilized SBA-15: Under extremely dry conditions, a suspension of CAL-immobilized SBA-15 (1 g) and hexamethyldisiloxane (HMDS) (0.1 mL) was heated at reflux overnight with stirring under nitrogen atmosphere. The volatiles were stripped on a rotary evaporator and the dry powder was washed two or three times with dry ethanol (10 mL) by centrifugation and finally dried under vacuum at 80 °C for 8 h. Greater than 98% of the material was recov-

ered. TMS capping of CAL-immobilized SBA-15 was confirmed by IR spectroscopy.

Asymmetric borane reduction of prochiral ketone catalyzed by CAL: CAL (82 mg, 7.34 mmol) was dissolved in dry tetrahydrofuran. Subsequently, borane dimethylsulfide (BMS) (0.15 mL, 2 mmol) was added by syringe and heated at reflux for 30 min to give chiral oxazaborolidine complex. Acetophenone (0.12 mL, 1 mmol) was added dropwise, and the mixture was again heated at reflux for 30 min. After completion of the reaction, the reaction mixture was quenched by the addition of 10 mL of 2 N HCl. The organic phase was extracted with dichloromethane, and the chiral secondary alcohol was separated by column chromatography on silica gel as adsorbent with 98:2 hexane/ethyl acetate as eluant.

Asymmetric borane reduction of prochiral ketone catalyzed by CAL-immobilized SBA-15: CAL-immobilized SBA-15 (140 mg, 30 mol%) was dissolved in dry toluene. BMS (0.12 mL, 1.5 mmol) was added by syringe and heated at reflux for 30 min to give chiral oxazaborolidine complex inside the mesoporous silica SBA-15. Subsequently, acetophenone (0.12 mL, 1 mmol) was added slowly. The reaction mixture was continuously heated at reflux for 30 min, cooled to room temperature, and filtered. To the filtrate was added 2 N HCl, and the mixture was extracted with dichloromethane. The chiral secondary alcohol was separated by column chromatography on silica gel as adsorbent with 98:2 hexane/ethyl acetate as an eluant.

Characterization of CAL-immobilized mesoporous SBA-15: The powder X-ray diffraction (XRD) patterns of CAL-immobilized SBA-15 samples were collected on a Rigaku diffractometer using $Cu_{K\alpha}$ ($\lambda = 0.154$ nm) radiation. The diffractograms were recorded in the 2θ range of 0.8 to 10° with a 2θ step size of 0.01° and a step time of 10 s. Nitrogen adsorption and desorption isotherms were measured at −196 °C on a Quantachrome Autosorb 1C sorption analyzer. All samples after the CAL immobilization were outgassed at 40 °C for 48 h. The specific surface area was calculated using the Brunauer–Emmett–Teller (BET) method. The pore size distributions were obtained from the adsorption branch of the nitrogen isotherms by Barrett–Joyner–Halenda method. ^{1}H and ^{13}C NMR spectra were recorded in $CDCl_3$ on a BRUKER AMX-300 MHz instrument using tetramethylsilane as an internal standard. Specific rotations were recorded with a Rudolph Autopol IV polarimeter. Enantiomeric excess was determined with a Shimadzu 2010 A HPLC instrument (Chiral column: Chiral Cel OD-H, mobile phase: hexane/isopropanol 98:2, 0.5 mL min^{-1}, 254 nm. FTIR spectra were recorded on a Perkin–Elmer - DXB spectrometer. Melting points of the chiral ligands were determined with a Kherea digital melting point apparatus and are reported uncorrected. The morphology of the materials before and after the chiral ligand immobilization was observed on a Hitachi S-4800 field emission scanning electron microscope using an accelerating voltage of 5.0 to 20 kV. The samples were deposited on a sample holder with an adhesive carbon foil and sputtered with platinum prior to imaging.

Acknowledgements

We thank the DST for financial assistance (SR/FTP/CS-142-2006) in the form of a fast track sponsored project and Dr. M. Chidambaram (Director, NITT) for constant encouragement, support, and research grants for U.B. and N.A. This work was also supported in part by the Ministry of Education, Culture, Sports, Science and Technology (MEXT) under the Strategic Program for Building an Asian Science and Technology Community Scheme and World Premier International Research Center (WPI) Initiative on Materials Nanoarchitectonics (MEXT, Japan).

[1] V. K. Singh, *Synthesis* **1992**, *7*, 605.
[2] S. Itsuno, K. Ito, A. Hirao, S. Nakahama, N. Yamazaki, *J. Chem. Soc. Chem. Commun.* **1983**, 469.
[3] S. Itsuno , K. Ito, *J. Org. Chem.* **1984**, *49*, 555.
[4] E. J. Corey, R. K. Bakshi, S. Shibata, *J. Am. Chem. Soc.* **1987**, *109*, 5551.
[5] E. J. Corey, G. A. Reichard, *Tetrahedron Lett.* **1989**, *30*, 5207.
[6] E. J. Corey, J. O. Link, *Tetrahedron Lett.* **1992**, *33*, 3431.
[7] E. J. Corey, C. J. Helal, *Tetrahedron Lett.* **1995**, *36*, 9153.
[8] C. J. Helal, P. A. Magriotis, E. J. Corey, *J. Am. Chem. Soc.* **1996**, *118*, 10938.
[9] B. Pugin, H. U. Blaser in *Comprehensive Asymmetric Catalysis*, *Vol. 3* (Eds.: E. N. Jacobsen, A. Pfaltz, H. Yamamoto), Springer, Berlin, **1999**, p. 367.
[10] J. A. David, P. Indra, R. S. David, *Chem. Rev.* **1996**, *96*, 835.
[11] X. Yao, H. Chen, W. Lu, G. Pan, X. Hu, Z. Zhen, *Tetrahedron Lett.* **2000**, *41*, 10267.
[12] G. J. Kim, J. H. Shin, *Tetrahedron Lett.* **1999**, *40*, 6827.
[13] S. H. Kim, J. Ong, S. T. Chung, M. J. Jin, *J. Ind. Eng. Chem.* **2001**, *7*, 259.
[14] S. W. Kim, S. J. Bae, T. Hyeon, B. M. Kim, *Microporous Mesoporous Mater.* **2001**, *44*, 523.
[15] N. Bellocq, D. Brunel, M. Lasperas, P. Moreau, *Stud. Surf. Sci. Catal.* **1997**, *108*, 485.
[16] M. S. Wang, Y. K. Kwon, G. J. Kim, *J. Ind. Eng. Chem.* **2002**, *8*, 262.
[17] D. Zhao, Q. Huo, J. Feng, B. F. Chmelka, G. D. Stucky, *J. Am. Chem. Soc.* **1998**, *120*, 6024.
[18] P. Yang, D. Zhao, D. Margolese, B. F. Chmelka, G. D. Stucky, *Nature* **1998**, *396*, 152.
[19] D. Zhao, J. Feng, Q. Huo, N. Melosh, G. H. Fredrickson, B. F. Chmelka, G. D. Stucky, *Science* **1998**, *279*, 548.
[20] S. J. Bae, S. W. Kim, T. Hyeon, *Chem. Commun.* **2000**, 31.
[21] S. Narasimhan, S. Swarnalakshmi, R. Balakumar, S. Velmathi, *Ind. J. Chem. Sec. B* **2002**, *41*, 1666.
[22] S. Narasimhan, S. Velmathi, R. Balakumar, V. Radhakrishnan, *Tetrahedron Lett.* **2001**, *42*, 719.
[23] S. Narasimhan, S. Swarnalakshmi, R. Balakumar, S. Velmathi, *Molecules* **2001**, *6*, 988.
[24] J. Xu, T. Wei, Q. J. Zhang, *J. Org. Chem.* **2003**, *68*, 10146.
[25] N. J. Gilmore, S. Jones, M. P. Muldowney, *Org. Lett.* **2004**, *6*, 2805.
[26] T. Fang, J. Xu, D. Du, *Synlett* **2006**, *10*, 559.

Received: September 1, 2009
Published online: January 15, 2010

